

## Efficient Thrombin Generation Requires Molecular Phosphatidylserine, Not a Membrane Surface

Rinku Majumder, Gabriel Weinreb, and Barry R. Lentz\*

Program in Molecular and Cellular Biophysics, Department of Biochemistry and Biophysics, University of North Carolina at Chapel Hill, Chapel Hill, North Carolina 27599-7260

Received July 26, 2005; Revised Manuscript Received October 11, 2005

**ABSTRACT:** Activation of prothrombin to thrombin is catalyzed by a “prothrombinase” complex, traditionally viewed as factor X<sub>a</sub> (FX<sub>a</sub>) in complex with factor V<sub>a</sub> (FV<sub>a</sub>) on a phosphatidylserine (PS)-containing membrane surface, which is widely regarded as required for efficient activation. Activation involves cleavage of two peptide bonds and proceeds via one of two released intermediates or through “channeling” (activation without the release of an intermediate). We ask here whether the PS molecule itself and not the membrane surface is sufficient to produce the fully active human “prothrombinase” complex in solution. Both FX<sub>a</sub> and FV<sub>a</sub> bind soluble dicaproyl-phosphatidylserine (C6PS). In the presence of sufficient C6PS to saturate both FX<sub>a</sub> and FV<sub>a2</sub> (light isoform of FV<sub>a</sub>), these proteins form a tight ( $K_d = 0.6 \pm 0.09$  nM at 37 °C) soluble complex. Complex assembly occurs well below the critical micelle concentration of C6PS, as established in the presence of the proteins by quasi-elastic light scattering and pyrene fluorescence. Ferguson analysis of native gels shows that the complex migrates with an apparent molecular mass only slightly larger than that expected for one FX<sub>a</sub> and one FV<sub>a2</sub>, further ruling out complex assembly on C6PS micelles. Human prothrombin activation by this complex occurs at nearly the same overall rate ( $2.2 \times 10^8$  M<sup>-1</sup> s<sup>-1</sup>) and via the same reaction pathway (50–60% channeling, with the rest via the meizothrombin intermediate) as the activation catalyzed by a complex assembled on PS-containing membranes ( $4.4 \times 10^8$  M<sup>-1</sup> s<sup>-1</sup>). These results question the accepted role of PS membranes as providing “dimensionality reduction” and favor a regulatory role for platelet-membrane-exposed PS.

Prothrombin is activated to thrombin in the final step of the blood coagulation cascade by an enzyme complex, called “prothrombinase” that consists of blood coagulation factors X<sub>a</sub> (FX<sub>a</sub>,<sup>1</sup> a serine protease) and V<sub>a</sub> (FV<sub>a</sub>, a cofactor), Ca<sup>2+</sup>, and negatively charged membranes (1, 2). The negatively charged membrane surface is provided by vesicles derived from activated platelets, upon which phosphatidylserine (PS) is exposed (3, 4). In the resting (i.e., “unactivated”) human platelet, PS is sequestered on the cytoplasmic leaflet of the platelet membrane (5). The classical view is that the PS-containing membrane surface provided by activated platelets favors both assembly of the enzyme–cofactor complex and diffusion of the membrane-associated substrate to the assembled complex because of a reduction from a three- to two-dimensional space (6–8) (the “surface dimensionality-reduction hypothesis”). Our laboratory postulates another view (the “regulatory PS hypothesis”) that PS occupancy of regulatory sites on both factors V<sub>a</sub> and X<sub>a</sub> produces confor-

mational changes that lead to tight association of these two proteins, both on a membrane and in solution. We suggest that these conformational changes alter both the pathway and rate of prothrombin activation. This hypothesis has evolved from examining the functional and structural consequences of the interaction of a soluble form of PS having short acyl chains (C6PS) with identified regulatory sites on both factors X<sub>a</sub> and V<sub>a</sub> (9–18).

Clearly, a critical test of these alternative hypotheses would be to compare the detailed kinetics of prothrombin activation by a prothrombinase complex assembled on a membrane surface with that seen for activation by a FX<sub>a</sub>–FV<sub>a</sub> complex assembled in the presence of C6PS in solution. If activation is possible in solution at a rate and by a reaction path comparable to that seen in the presence of membranes, it would offer strong support for the “regulatory PS hypothesis” and would be inconsistent with the “surface dimensionality-reduction” hypothesis. As a key step toward the goal of comparing the solution- and membrane-assembled complex, we showed that C6PS triggers tight binding between bovine factors X<sub>a</sub> and V<sub>a</sub> to create a highly active prothrombin-activating complex in solution (16). However, Stone and Nelsestuen recently reported that an efficient human prothrombinase complex could not be triggered in solution by C6PS and that “high activity only occurred under conditions where a membrane bilayer was present” (19). Could the prothrombinase from these two similar species be so different? Here, we show that C6PS does trigger a soluble human

\* To whom correspondence should be addressed. Telephone: 919-966-5384. Fax: 919-966-2852. E-mail: uncbrl@med.unc.edu.

<sup>1</sup> Abbreviations: DAPA, dansylarginine-*N*-(3-ethyl-1,5-pentanediy)-amide; SDS–PAGE, sodium dodecyl sulfate–polyacrylamide gel electrophoresis; PEG, poly(ethylene glycol); S-2238, *H*-D-phenylalanyl-L-pipecolyl-L-arginine-*p*-nitroaniline dihydrochloride; S-2765, *N*-α-benzyloxycarbonyl-D-arginyl-L-glycyl-L-arginine-*p*-nitroaniline dihydrochloride; DOPC, 1,2-dioleoyl-3-*sn*-phosphatidylcholine; C6PS, 1,2-dicaproyl-*sn*-glycero-3-phospho-L-serine; PS, phosphatidylserine; FX<sub>a</sub>, factor X<sub>a</sub>; FV<sub>a</sub>, factor V<sub>a</sub>; Pre2, prethrombin 2; II<sub>a</sub>, thrombin; MzII<sub>a</sub>, meizothrombin; F1.2, fragment 1.2.

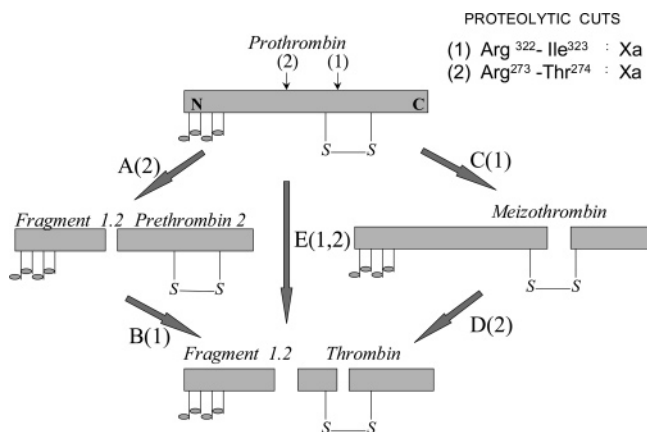


FIGURE 1: Schematic representation of human prothrombin (II) activation. Two peptide bonds (23) and {Arg<sup>322</sup>–Ile<sup>323</sup>} in prothrombin must be cut by FX<sub>a</sub> for activation to thrombin (II<sub>a</sub>). This creates two possible pathways of activation (A and B, and C and D) and two possible released intermediates (Pre2 and MzII<sub>a</sub>). A third possible pathway of activation (E) occurs when no intermediate is released (“channeling” or processive activation).

X<sub>a</sub>–V<sub>a</sub> complex in solution when published precautions are taken to reduce absorption of coagulation proteins to glass surfaces and when poly(ethylene glycol) (PEG) rather than bovine albumin (a lipid-binding protein) is used as a protein-stabilizing agent.

Analysis of the kinetics of prothrombin activation by a FX<sub>a</sub>–FV<sub>a</sub> complex is not simple because prothrombin activation can proceed via two possible proteolytic intermediates, meizothrombin [MzII<sub>a</sub>; probably the major intermediate *in vivo* (20)] and prethromin2 plus fragment 1.2 (Pre2 + F1.2; Figure 1) (21–23). In addition, both FV<sub>a</sub> (24) and PS membranes (14, 25) stimulate activation via a path that results in thrombin formation without the release of an intermediate (“channeling”, reaction E in Figure 1). Other complications are that (1) the reaction product (thrombin) and one of the intermediates (MzII<sub>a</sub>) have similar proteolytic activities, (2) the other intermediate (Pre2 + F1.2) has little or no activity, and (3) intermediates are consumed at rates comparable to those at which they are produced. Because of these complications, our initial demonstration of a C6PS-assembled bovine X<sub>a</sub>–V<sub>a</sub> complex in solution did not establish the kinetic pathway for activation of prothrombin by this complex (i.e., the extent of channeling and the rates of individual bond cleavages). In this paper, we present a complete kinetic analysis of the human complex assembled in solution by C6PS and show this to be nearly identical to the complex assembled on a membrane surface. In this way, we show that the “surface dimensionality-reduction” hypothesis does not explain the effect of PS-containing membranes on prothrombin activation. Our results thereby offer strong support for the “regulatory PS” hypothesis.

## MATERIALS AND METHODS

**Materials.** Ecarin from *Echis carinatus* snake venom, heparin, and EGTA were purchased from Sigma Chemical Company (St. Louis, MO). Dansylarginine-*N*-(3-ethyl-1,5-pentanedyl)amide (DAPA) was obtained from Hematologic Technologies Inc. (Essex Junction, VT). The thrombin-specific substrate, S-2238, and the factor X<sub>a</sub> substrate, S-2765, were purchased from AB Kabi Diagnostica (Moln-

dal, Sweden). 1,2-dicaproyl-*sn*-glycero-3-phospho-L-serine (C6PS), porcine brain phosphatidylserine (PS), and 1,2-dioleoyl-3-*sn*-phosphatidylcholine (DOPC) were purchased from Avanti Polar Lipids Inc. (Alabaster, AL), and stock solutions were prepared from the purchased chloroform stock as described before (11). Human prothrombin and factor X<sub>a</sub> and Pre2 + F1.2 were obtained from Hematologic Technologies Inc. (Essex Junction, VT), and MzII<sub>a</sub> (26) and [5-(dimethylamino)-1-naphthalenesulfonyl] glutamylcylarginyl chloromethyl ketone (DEGR)-labeled factor X<sub>a</sub> (16) were prepared as described. Prothrombin was activated to thrombin with Taipei venom and assayed with synthetic substrate S-2238, using an active-site-titrated thrombin standard. Factor X<sub>a</sub> was assayed using S-2765 substrate, again using an active-site-titrated standard. Purified human factor V was prepared from fresh frozen human plasma (American Red Cross Center, Durham, NC) and then activated to factor V<sub>a</sub> as described previously according to refs 27 and 28. The activity of FV<sub>a</sub> was assayed using 25:75 PS/DOPC vesicles (29). Human FV<sub>a</sub> has two natural isoforms (30) resulting from differential glycosylation at Asp2181 in the C2 domain (31). Only the unglycosylated form (FV<sub>a2</sub>) binds with nanomolar affinity to FX<sub>a</sub> in the presence of C6PS in solution (16, 31). Human FV<sub>a2</sub> was separated from FV<sub>a1</sub> (the heavy isoform) by HPLC chromatography on a Mono-S column (Pharmacia, now Pfizer, NY) as described (15, 31). All experiments on the prothrombin-activating complex in solution used FV<sub>a2</sub>. All proteins were further tested for purity by sodium dodecyl sulfate–polyacrylamide gel electrophoresis (SDS–PAGE, 1 μg of loading on minigels) using nonreducing and reducing conditions. No impurities were detected in prothrombin or FX<sub>a</sub>, and the density of a slight impurity in FV<sub>a2</sub> was <5% of that of the main FV<sub>a2</sub> band. Purified (32) PEG (0.6 wt %, PEG 8000 from Fisher Scientific, Fairlawn, NJ) was used as a protein-stabilizing agent.

**Methods: Critical Micelle Concentration (cmc) Determination.** Key controls for the occurrence of C6PS micelles were performed by measuring the diameters of aggregates using quasi-elastic light scattering (9). This method is capable of detecting both the minimal micelles formed by pure C6PS [*N* ~ 200 (9)] as well as the larger aggregates formed in the presence of prothrombin, FX<sub>a</sub>, FV<sub>a</sub>, or a combination of these proteins (9, 15, 16). Changes in pyrene fluorescence (33) were also used to document the cmc of C6PS. This probe is very hydrophobic and partitions strongly into hydrophobic environments. It has a complex fluorescence spectrum that is sensitive to the polarity of its environment. The ratio of the intensity of the pyrene emissions at 373 and 383 nm, defined as *I*<sub>1</sub>/*I*<sub>3</sub>, provides information on the polarity of the microenvironment of the probe. Pyrene fluorescence has been shown to detect micelles with aggregation numbers as small as 10, as validated by a comparison to cmc determination by surface tension and conductivity measurements (33, 34), the two measures of micelle formation widely recognized as most sensitive.

**Preparation of Phospholipid Vesicles.** Extruded unilamellar vesicles (diameter ~ 110 nm) composed of 25:75 bovine PS/DOPC were prepared, and the phospholipid concentration was determined, as described previously (14).

**Fluorescence Stopped-Flow Measurements.** The rates of thrombin formation from either MzII<sub>a</sub> or Pre2 (with equimolar fragment 1.2) or of thrombin plus MzII<sub>a</sub> formation from

human prothrombin were estimated from the time-dependent fluorescence change of DAPA bound to the activation products. The use of DAPA for this purpose was pioneered by Mann et al. (35, 36), and prothrombin activation rates measured by this method in the presence of PS-containing membranes were shown to be equivalent to rates measured either with thrombin-specific substrates or with quantitative SDS–PAGE (14, 25). Stopped-flow measurements were performed using an SLM-Aminco Milliflow stopped-flow reactor (Spectronic Instruments, Inc., Rochester, NY) attached to the SLM 48 000 spectrofluorometer (Spectronic Instruments), as described previously in detail (14, 25). One syringe contained substrate solution and DAPA in 20 mM Tris, 150 mM NaCl, 5 mM CaCl<sub>2</sub> at pH 7.5, and 0.6% PEG, and the other syringe contained pre-assembled prothrombinase (FX<sub>a</sub>, FV<sub>a</sub>, and C6PS) in the same buffer, with the final concentrations of factors X<sub>a</sub> and V<sub>a2</sub> in the reaction chamber being 1 and 5 nM and the substrate/DAPA ratio being 1:5. Both syringes were maintained at 37 °C as was the mixing chamber. The calculation of rates from measurements of initial fluorescence intensity ( $F_0$ ) and intensity at the completion of the reaction ( $F_\infty$ ) is described elsewhere (14, 22). For all experiments involving the assembly of the FV<sub>a2</sub>–FX<sub>a</sub> complex in the absence of membranes, the reaction chambers (stopped-flow or quench-flow mixing chambers or cuvettes) were pretreated with an appropriate solution of FX<sub>a</sub>, FV<sub>a2</sub>, and C6PS and then rinsed with buffer before performing the reaction, as previously noted (16). Failure to condition surfaces in this way led to irreproducible results, because of protein absorption to quartz surfaces during experiments, an artifact likely to be most significant at low protein concentrations. A buffer blank was obtained with the conditioned cuvette/stop-flow chamber prior to each experiment.

**Rapid Chemical-Quench Measurements.** Rapid quench experiments were performed using the Chemical-Quench-Flow Model RQF-3 from Kintek Corp. (State College, PA) as described in detail elsewhere (14, 25). The temperature was maintained at 37 °C. The buffer contained 20 mM Tris, 150 mM NaCl, and 5 mM Ca<sup>2+</sup> with 0.6% PEG. The mixture was expelled from the Quench-Flow instrument into a collection tube after the reaction was complete. Aliquots from collected samples were assayed for amidolytic activity using S-2238 in a VersaMax microplate reader (Molecular Devices Corp., Sunnyvale, CA) that was pretreated with 0.6 wt % PEG and air-dried to prevent sticking of the proteins to the micro plate. The concentration of active site (II<sub>a</sub> plus MzII<sub>a</sub>) was determined by comparing the initial rate of S-2238 hydrolysis to a standard curve, as described by Wu et al. (14). To measure the amount of MzII<sub>a</sub> formed, the amidolytic activity was measured after incubating the reaction mixture aliquot for 1 min in the presence of heparin (10 µg/mL) and anti-thrombin III (300 nM), thereby blocking the thrombin but not the MzII<sub>a</sub> active site (37). The initial rate of thrombin formation was obtained by subtracting the rate of MzII<sub>a</sub> appearance from the initial rate of total active-site formation.

**Fluorescence Titration of DEGR-X<sub>a</sub> by FV<sub>a2</sub>.** These measurements were carried out with the SLM 48 000 spectrofluorometer (SLM Aminco, Urbana, IL) as described previously in detail (16).

**Analysis of Prothrombin Activation by SDS–PAGE.** Reaction mixtures were as described for the chemical-quench

experiments. Aliquots of 40 µL were taken at 0.5, 0.75, 1, 1.25, and 1.5 s and subjected to gel electrophoresis (1.5 mm of 12% polyacrylamide) with and without reduction with 5% (v/v) 2-mercaptoethanol (38). Protein bands were visualized by staining with Colloidal Coomassie blue (39), and protein bands were quantitated as described in detail previously (14, 25).

**Native Gel Electrophoresis.** Procedures were described in detail previously (16, 17). A mixture of 5 nM FX<sub>a</sub> and 5 nM FV<sub>a2</sub>, also in the buffer used for kinetics, was incubated at a controlled temperature for 2 min in the presence and absence of 400 µM C6PS, and these two samples were run together with known marker proteins (270–14.2 kDa; Sigma, St. Louis, MO) on five gels (5, 6, 6.5, 7, and 8% total acrylamide, with bisacrylamide/acrylamide being 1:29 in all cases) in a BioRad Mini-Protean II minigel apparatus (Biorad Corp., Hercules, CA) and stained with colloidal Coomassie blue (39). FX<sub>a</sub> and FV<sub>a</sub>, at these same concentrations and in the presence of 400 µM C6PS, were run separately as controls.

**Data Analysis: FV<sub>a2</sub>–FX<sub>a</sub> Binding.** The total concentration of the DEGR-X<sub>a</sub>·V<sub>a</sub> complex at any given C6PS concentration ( $[DEGR-X_a \cdot V_a]_{(C6PS)}$ ) is given by the familiar expression for two species binding

$$[DEGR-X_a \cdot V_a]_{(C6PS)} = [DEGR-X_a]_{tot} + [V_a]_{tot} + K_d^{eff} - \sqrt{([DEGR-X_a]_{tot} + [V_a]_{tot} + K_d^{eff})^2 - 4[DEGR-X_a]_{tot}[V_a]_{tot}}/2 \quad (1)$$

where the concentration terms all are “total” concentrations of each species in a sample. The change in fluorescence signal of DEGR-X<sub>a</sub> was taken as proportional to the fraction of DEGR-X<sub>a</sub> bound to FV<sub>a</sub>

$$\frac{F - F_0}{F_{SAT} - F_0} = \frac{[DEGR-X_a \cdot V_a]_{(C6PS)}}{[DEGR-X_a]_{tot}} \quad (2)$$

where the fluorescence parameter  $F_0$  was fixed as the DEGR-X<sub>a</sub> fluorescence before titration began and  $F_{SAT}$  is the fluorescence at saturation, which was obtained along with  $K_d$  by nonlinear regression of the data as described in ref 16.

**Kinetic Analysis.** To determine the kinetic constants for the first two proteolytic events (reactions A and C, see Figure 1), three experimentally determined time courses (thrombin formation, MzII<sub>a</sub> appearance, and Pre2 appearance) were fitted according to a parallel, sequential reaction scheme (Figure 1) (14). A fraction,  $f$ , of prothrombin was considered to convert directly (i.e., channel) to thrombin without the escape of an intermediate from the lipid–enzyme–cofactor complex (14, 24, 25). All three sets of data were fitted simultaneously by adjusting first-order rate constants  $R_A$  (for reaction A, Figure 1),  $R_C$  (reaction C), and  $R_E$  (reaction E), while  $R_B$  and  $R_D$  (for reactions B and D) were fixed at the values determined independently in this paper. Competition of prothrombin and MzII<sub>a</sub> substrates for enzyme active sites was explicitly taken into account by estimating the fraction of enzyme tied up with prothrombin using the measured  $K_M$  for MzII<sub>a</sub> or Pre2 + F1.2 activation to prothrombin (~0.6–0.7 nM) (14). Global fitting of the data



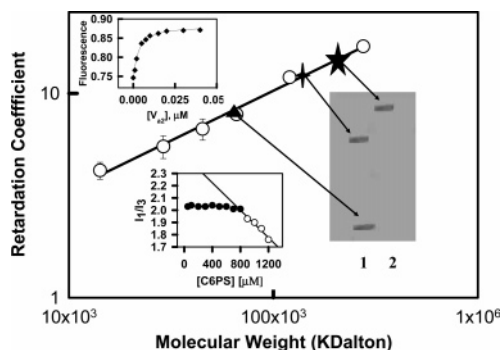


FIGURE 2: Characterization of the complex formed by FX<sub>a</sub> and FV<sub>a2</sub> in the presence of soluble C6PS. The retardation coefficients of several reference proteins obtained from native polyacrylamide gel electrophoresis on a 6% gel (16) are plotted in a log–log fashion versus the molecular mass (○). Points have been added to this plot for retardation coefficients obtained for 5 nM FX<sub>a</sub> (▲) or 5 nM FV<sub>a2</sub> (four pointed star) in the absence of C6PS and of the 5 nM FX<sub>a</sub>·FV<sub>a2</sub> complex (★) formed in the presence of 400 μM C6PS, (the buffer was 20 mM Tris, 150 mM NaCl, and 5 mM CaCl<sub>2</sub> at pH 7.5) at 22 °C in the absence (lane 1) and presence (lane 2) of C6PS. The lower inset illustrates determination of the C6PS critical micelle concentration by pyrene fluorescence under the conditions of these experiments. The abrupt appearance of aggregates above 800 μM C6PS defines the critical micelle concentration under these experimental conditions as 770 ± 4 μM. The change in fluorescence intensity of active-site-labeled 1 nM human FX<sub>a</sub> (DEGR-X<sub>a</sub>) with the addition of FV<sub>a2</sub> (◆) in the presence of 400 μM C6PS at 22 °C is plotted in the upper inset, yielding a dissociation constant ( $K_d$ ) of 2 ± 0.2 nM.

using the SCoP Simulation Program (Simulations Resources Inc., Berrin Springs, MI) was described previously (14).

## RESULTS

**Thermodynamics of FV<sub>a</sub>–FX<sub>a</sub> Complex Assembly.** Although we have documented the C6PS-induced tight association of bovine factors V<sub>a2</sub> and X<sub>a</sub> in solution (16), we had to characterize the C6PS-induced association of human proteins before determining the catalytic properties of this enzyme complex. As we have reported for bovine factors X<sub>a</sub> and V<sub>a</sub>, (16), the two isoforms of human FV<sub>a</sub> have very different abilities to interact with FX<sub>a</sub> in the presence of C6PS. The upper inset of Figure 2 documents the association of DEGR-X<sub>a</sub> with FV<sub>a2</sub> in the presence of 400 μM C6PS at 22 °C. Analysis of these data by a simple 1:1 binding model gave a  $K_d$  of 2.0 ± 0.2 nM, compared to binding of FV<sub>a1</sub> to FX<sub>a</sub> with a  $K_d$  of >1 μM in the absence of C6PS (data not shown). We performed similar titrations of DEGR-X<sub>a</sub> with FV<sub>a2</sub> at 37 °C (where we made functional measurements) and at 12 °C and found  $K_d$  values of 0.6 ± 0.09 nM at 37 °C and 4.1 ± 0.2 nM at 12 °C. From these equilibrium constants, we determined  $\Delta H$ ,  $\Delta G$ , and  $T\Delta S$  for FX<sub>a</sub>–FV<sub>a2</sub> binding at 12, 22, and 37 °C using the Gibbs–Helmholtz equation. Because the plot of  $\ln K_d$  versus 1/ $T$  was linear over this range,  $\Delta H$  was temperature-invariant (5 ± 0.4 kcal/mol).  $\Delta G$  and  $T\Delta S$  were –13.5 ± 1 and 18.5 ± 0.8 kcal/mol at 37 °C, –11.7 ± 0.5 and 16.7 ± 1 kcal/mol at 22 °C, and –3.3 ± 0.7 and 8.3 ± 0.9 kcal/mol at 12 °C. The interaction of FX<sub>a</sub> with FV<sub>a2</sub> is thus entropically driven. These results are consistent with FX<sub>a</sub>–FV<sub>a2</sub> binding having a significant hydrophobic interaction component, although certain salt bridges would also be consistent with our data.

**Do C6PS Aggregates Contribute to FV<sub>a</sub>–FX<sub>a</sub> Complex Formation?** Because FV<sub>a</sub> is believed to bind tightly to FX<sub>a</sub> only on a membrane surface (40), we must ask whether the tight binding observed between FV<sub>a2</sub> and FX<sub>a</sub> could be due to FV<sub>a2</sub> and FX<sub>a</sub> bound to a C6PS aggregate or micelle. We have directly determined the size of aggregates detected at different C6PS concentrations under the conditions used for our kinetic experiments (1 nM FX<sub>a</sub> and 5 nM FV<sub>a2</sub> and 1 μM prothrombin) by quasi-elastic light scattering (9). From this, we determined the cmc of C6PS in the presence of factors X<sub>a</sub> and V<sub>a2</sub> to be roughly 700–750 μM. No aggregates were detectable at or below 700 μM, even though micelles containing only 200 C6PS molecules are revealed by this method (9). The cmc determined by this method agrees well with that determined by an indirect but more sensitive method, pyrene fluorescence (lower inset to Figure 2, 770 ± 4 μM). Pyrene fluorescence detects micelles with aggregation numbers as low as 10 (33, 34). Changes {1} in factor X<sub>a</sub> activity (9), {2} in the fluorescence of surface-seeking fluorescence probes (9), and {3} in CD spectra of factor X<sub>a</sub> (17) are also detected at the cmc measured by these methods. Similar experiments have shown that the C6PS cmc is even higher in the presence of FV<sub>a2</sub> or FX<sub>a</sub> individually (9, 15). In agreement with this, equilibrium dialysis shows that FV<sub>a</sub> and FX<sub>a</sub> bind only 4 and 2 C6PS molecules/protein molecule, respectively, below the measured cmc values (12, 15). Thus, our experiments (carried out at ≤400 μM C6PS) are all performed well below the cmc of C6PS under our experimental conditions.

As another measure of aggregate formation, we examined the hydrodynamic size of the FV<sub>a</sub>–FX<sub>a</sub> complex by native gel electrophoresis of 5 nM FX<sub>a</sub> and FV<sub>a2</sub> in the absence (lane 1) and presence (lane 2) of C6PS at 22 °C (gel in Figure 2). This gel clearly shows the appearance of a complex (~65% of the total protein based on digitizing the stained gel) (★) in the presence of 400 μM C6PS. In the absence of C6PS, no complex appeared (lane 1 in Figure 2). This result confirms that FV<sub>a2</sub> and FX<sub>a</sub> form a well-defined complex in the presence of C6PS. The fraction of unbound FV<sub>a2</sub> and FX<sub>a</sub> (~35%) under these conditions compares well with that calculated (~40%) using the  $K_d$  measured for DEGR-X<sub>a</sub> at 22 °C, demonstrating that the gel method reports close to the equilibrium mixture of monomers and complex that was applied to the gel. This is consistent with reports that macromolecular complexes dissociate slowly on gels (because of sequestering of the complex in a small volume) (41). Similar gels run at 37 °C (where our kinetic analysis was done) showed that virtually all FX<sub>a</sub> and FV<sub>a2</sub> were incorporated into complex, as predicted from the  $K_d$  determined at this temperature.

Ferguson analysis uses measured  $R_f$  values for a protein on gels of different cross-linking densities to obtain a mobility parameter (retardation coefficient) dependent upon hydrodynamic radius and shape but independent of charge (42). For globular proteins of roughly spherical shape, this method yields good estimates of molecular size by comparing the retardation coefficient of an unknown protein to those of a standard set of globular proteins of known molecular size. If all proteins under consideration are similarly packed and have roughly the same molar density, it is appropriate to express molecular size in terms of the apparent molecular mass. Figure 2 shows a Ferguson plot (43) of retardation

coefficients versus the molecular mass of standard proteins along with points added for FX<sub>a</sub> (▲) and FV<sub>a2</sub> (four pointed star) and the FX<sub>a</sub>–FV<sub>a2</sub> complex (★). On the basis of this Ferguson analysis, the FX<sub>a</sub>•FV<sub>a2</sub>•C6PS complex that we have detected by PAGE has an *apparent* molecular mass of  $224 \pm 3.7$  kDa, while the apparent molecular masses of FX<sub>a</sub> (▲) and FV<sub>a2</sub> (◆) were estimated as  $46 \pm 1.2$  and  $176.5 \pm 2$  kDa, respectively. Reported molecular masses of FX<sub>a</sub> and FV<sub>a2</sub> are 46 kDa (44) and 177 kDa (27), respectively, showing that Ferguson analysis, along with our assumptions about molecular density and shape, gives reasonable estimates of the molecular masses of both proteins and thus should do so for their complex. The apparent molecular mass of the complex ( $224 \pm 3.7$  kDa) is consistent with that expected for a 1:1 complex of FX<sub>a</sub> with FV<sub>a2</sub> (222 kDa, on the basis of our measurements of these proteins individually, or 223 kDa, on the basis of published individual molecular masses). Assuming that the molar density of C6PS is comparable to that of globular proteins, this finding is inconsistent with incorporation of a large number ( $\geq 20$ , derived from measured experimental errors) of C6PS molecules into the FX<sub>a</sub>–FV<sub>a2</sub> complex.

**Kinetics of Prothrombin Activation.** Because prothrombin can be activated by three possible pathways (Figure 1), we must characterize five possible proteolytic steps. Two of these create the intermediates MzII<sub>a</sub> and Pre2 + F1.2 (reactions C and A in Figure 1), and two of these (reactions B and D) convert the intermediates to thrombin. A fifth reaction (reaction E in Figure 1) converts prothrombin to thrombin without the release of an intermediate (channeling or processive activation) (14, 24, 25). We characterized all of these reactions for the C6PS-assembled prothrombinase using the same approach applied in published studies of the kinetics of prothrombin activation by factor X<sub>a</sub> alone (no factor V<sub>a</sub>), factor X<sub>a</sub> in the presence either of C6PS (11) or of PS-containing membranes (14), and the FV<sub>a2</sub>–FX<sub>a</sub> complex assembled on PS-containing membranes (25). Note that C6PS binds very weakly to two sites in the Kringle domains of prothrombin (linked  $K_d$  values of  $28 \mu\text{M}$  and  $5 \text{ mM}$ ; Sen, Banerjee, Zhou, Majumder, and Lentz, unpublished results), meaning that C6PS should not bind significantly to these substrates at the substrate concentrations ( $1\text{--}5 \mu\text{M}$ ) used in our kinetic studies. The time courses of thrombin formation from MzII<sub>a</sub> (reaction B) or Pre2 + F1.2 (reaction D) as catalyzed by  $1 \text{ nM}$  FX<sub>a</sub> and  $5 \text{ nM}$  FV<sub>a2</sub> ( $K_d \sim 0.6 \text{ nM} \Rightarrow \sim 95\%$  of total FX<sub>a</sub> in complex) were determined by stopped-flow experiments as described in the Materials and Methods. The rates of MzII<sub>a</sub> and Pre2 + F1.2 activation by the soluble complex at this concentration are comparable to the very fast rates observed for  $2.5 \text{ nM}$  complex assembled in the presence of PS-containing membranes (25), making stopped-flow methods necessary. Plots of initial rates of thrombin formation versus the substrate concentration at different lipid concentrations (Figure 3) yielded  $K_M$  (■) and  $V_{\text{max}}$  (▲) for MzII<sub>a</sub> (inset of Figure 3A) and Pre2 + F1.2 (inset of Figure 3B) activation. To compare this C6PS-assembled FV<sub>a</sub>–FX<sub>a</sub> complex to the published kinetic behavior of the membrane-assembled prothrombinase, we needed second-order rate constants ( $k_{\text{cat}}/K_M$ ). To calculate these from  $V_{\text{max}}/K_M$ , we estimated the fraction of total FX<sub>a</sub> incorporated into prothrombinase ( $\sim 95\%$ ) from the  $K_d$  for the FX<sub>a</sub>–FV<sub>a2</sub> inter-

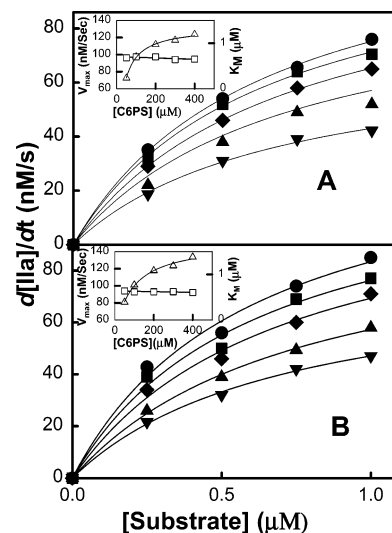


FIGURE 3: Initial rates of thrombin formation from intermediates as a function of the substrate concentration. Activation of MzII<sub>a</sub> (A) or an equimolar mixture of Pre2 + F1.2 (B) was initiated by stopped-flow mixing of equal volumes of the substrate and DAPA in one syringe with the FV<sub>a</sub>–FX<sub>a</sub> complex in another syringe ( $5 \text{ nM}$  FV<sub>a2</sub> and  $1 \text{ nM}$  FX<sub>a</sub> in a final reaction mixture). The concentrations of C6PS in the reactions were  $50 \mu\text{M}$  (▼),  $100 \mu\text{M}$  (▲),  $200 \mu\text{M}$  (◆),  $300 \mu\text{M}$  (■), and  $400 \mu\text{M}$  (●). The kinetic parameters  $V_{\text{max}}$  (Δ) and  $K_M$  (□) for the conversion of MzII<sub>a</sub> and Pre2 + fragment 1.2 to thrombin are plotted versus the C6PS concentration in the insets to A and B, respectively.

action ( $0.6 \text{ nM}$ ). Effective  $k_{\text{cat}}$  values were calculated as  $V_{\text{max}}/K_M$ , leading to the  $k_{\text{cat}}/K_M$  values given in Table 1.

To complete our kinetic analysis of the C6PS-assembled FV<sub>a</sub>–FX<sub>a</sub> complex, we needed rate constants for the initial steps shown in Figure 1 (reactions A and C) as well as for the channeling pathway (reaction E). To obtain these, we followed the approach that we used earlier to analyze the kinetics of prothrombin activation by membrane-bound factor X<sub>a</sub> (14) or the membrane-assembled FV<sub>a</sub>–FX<sub>a</sub> complex (25). Figure 4A shows initial time courses of thrombin (○ and ●) and MzII<sub>a</sub> (□ and ■) appearance measured by synthetic substrate assay (● and ■) as well as these time courses and that of Pre2 appearance (△) measured by SDS–PAGE (○ and □). The rate of thrombin formation was greater than the rate of MzII<sub>a</sub> appearance at  $400 \mu\text{M}$  C6PS ( $49.9 \text{ nM II}_a/\text{s}$  and  $30.6 \text{ nM MzII}_a/\text{s}$ ). The same behavior was noted previously for prothrombin activation by membrane-associated prothrombinase (25). As long as our experiments catch the initial steady-state kinetics of activation, this observation implies (14, 25) either that significant thrombin formation occurred through the Pre2 pathway or that a large fraction of MzII<sub>a</sub> and/or Pre2 was rapidly processed directly to thrombin (pathway E in Figure 1) and thus not detected as a released intermediate. Because no Pre2 formation was detected, we rule out the first possibility and conclude that a fraction of intermediate(s) is processed directly to thrombin (channeling).

Because DAPA is a weak competitive inhibitor of FX<sub>a</sub> (35), we tested whether results obtained with this thrombin-active-site fluorescent detector are consistent with results obtained by other methods. Thus, we calculated the expected DAPA fluorescence based on the time courses of thrombin and MzII<sub>a</sub> appearance (Figure 4) (14). The results are shown in the inset to Figure 4A (●) along with an experimental

Table 1: Kinetic Parameters ( $k_{\text{cat}}/K_M$ ) for Activation of Prothrombin and Its Intermediates<sup>a</sup>

enzyme	II $\rightarrow$ Pre2, F1.2 reaction A	II $\rightarrow$ MzII <sub>a</sub> reaction C	Pre2, F1.2 $\rightarrow$ II <sub>a</sub> reaction B	MzII <sub>a</sub> $\rightarrow$ II <sub>a</sub> reaction D	II $\rightarrow$ II <sub>a</sub> reaction E (channeling)
X <sub>a</sub> + Ca <sup>2+</sup> (14)	68	44	86	$1.1 \times 10^3$	0
X <sub>a</sub> + Ca <sup>2+</sup> + C6PS (11)	<400 <sup>b</sup>	$8.9 \times 10^3$	$1.7 \times 10^5$	$6.5 \times 10^5$	0
X <sub>a</sub> + Ca <sup>2+</sup> + C6PS + V <sub>a2</sub> (this paper)	0 <sup>b</sup>	$1.0 \pm 0.2 \times 10^8$	$3.0 \pm 0.4 \times 10^8$	$2.5 \pm 0.5 \times 10^8$	$1.4 \pm 0.4 \times 10^8$
X <sub>a</sub> + Ca <sup>2+</sup> + V <sub>a</sub> + PS/PC (25)	0 <sup>b</sup>	$0.59 \times 10^8$	$0.26 \times 10^8$	$0.29 \times 10^8$	$0.65 \times 10^8$

<sup>a</sup> All rate constants are in units of  $\text{M}^{-1} \text{s}^{-1}$ . <sup>b</sup> This reaction is too slow to be documented while the other, much faster reactions occur.

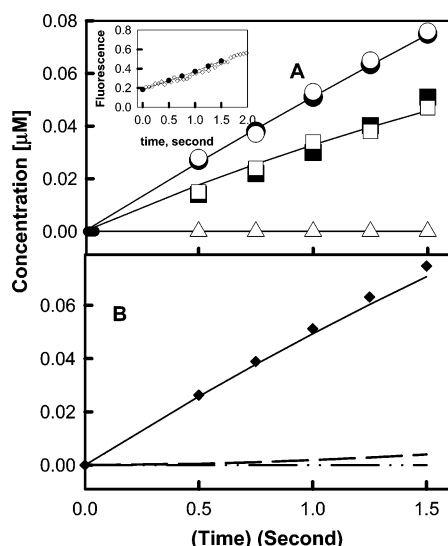


FIGURE 4: (A) Best fits of simulations to observed initial prothrombin proteolysis time courses. Prothrombin ( $0.5 \mu\text{M}$ ) proteolysis catalyzed by FX<sub>a</sub> ( $1 \text{ nM}$ ) in the presence of  $5 \text{ mM CaCl}_2$ , FV<sub>a2</sub> ( $5 \text{ nM}$ ), and  $400 \mu\text{M}$  C6PS, was monitored at  $37^\circ\text{C}$  either by means of thrombin (●) and MzII<sub>a</sub> (■) activity using synthetic substrates or by means of SDS–PAGE and densitometry (○ and □). The inset to A shows calculated DAPA fluorescence based on the results obtained with synthetic substrates (●) along with an experimental time course of DAPA fluorescence change (◇) reflecting prothrombin activation. (B) Calculated (on the basis of kinetic constants in Table 1) time courses of thrombin formed via the Pre2 (---), the MzII<sub>a</sub> (---), and the channeling (—) pathways at  $1 \text{ nM FX}_a$ ,  $5 \text{ nM FV}_{a2}$ ,  $0.5 \mu\text{M}$  prothrombin, and  $400 \mu\text{M}$  C6PS, with ◆ showing the experimental time course for total thrombin formation under these conditions.

time course of DAPA fluorescence change (◇) reflecting prothrombin activation. Similar results were obtained at the other prothrombin concentrations examined. From these results, it is clear that the presence of DAPA did not measurably inhibit FX<sub>a</sub> activity under our conditions.

To determine quantitative estimates of rate constants for reactions C and E, we fit globally all of the data in Figure 4A as described previously (14, 25), with rate constants for reactions B and D fixed at the measured values shown in Table 1. The second-order rate constants for reactions A, C, and E were adjusted to give the best fit (shown as — in Figure 4A), with the resulting values given in Table 1. The fraction of prothrombin converted to thrombin by channeling ( $\sim 0.58$ ) is given by the ratio of the rate of reaction E to the sum of rates of reactions A, C, and E.

Despite similarities in the channeling fractions [ $0.52$  on membranes (25) versus  $0.58$  with C6PS-assembled prothrombinase], activation was surprisingly roughly an order of magnitude faster for the C6PS-assembled complex than we have reported for the membrane-assembled human complex (25). This could be because the C6PS-assembled

complex is actually more active or because FV<sub>a2</sub> is a somewhat better cofactor in solution than is the natural FV<sub>a1</sub>–FV<sub>a2</sub> mixture previously examined on a membrane. To distinguish between these possibilities, we compared the initial rates of thrombin plus MzII<sub>a</sub> formation from prothrombin in the presence of soluble C6PS and 25% PS/DOPC 110-nm vesicles under identical experimental conditions but with either whole FV<sub>a</sub> or FV<sub>a2</sub> as cofactors. The overall  $k_{\text{cat}}/K_M$  estimated from these measurements for prothrombin activation by FX<sub>a</sub> and FV<sub>a2</sub> in the presence of C6PS ( $2.2 \times 10^8 \text{ M}^{-1} \text{s}^{-1}$ ) was only 2-fold smaller than in the presence of membranes ( $4.4 \times 10^8 \text{ M}^{-1} \text{s}^{-1}$ ). Overall activation by the membrane-prothrombinase-containing FV<sub>a2</sub> was roughly 40-fold faster than for the membrane-prothrombinase-containing FV<sub>a</sub> ( $k_{\text{cat}}/K_M \sim 10^7 \text{ M}^{-1} \text{s}^{-1}$ ), confirming that FV<sub>a2</sub> is a somewhat better cofactor than the natural mixture, even on a membrane, consistent with previous titrations of a mixture of FX<sub>a</sub> and either FV<sub>a2</sub> or FV<sub>a1</sub> with C6PS (16, 18). To make another comparison of the activities of the FV<sub>a2</sub> and FV<sub>a</sub> cofactors, we also compared the rates of MzII<sub>a</sub> activation by FX<sub>a</sub> on PS/DOPC membranes in the presence of FV<sub>a2</sub> ( $3.0 \times 10^8 \text{ M}^{-1} \text{s}^{-1}$ ) or FV<sub>a</sub> ( $2.9 \times 10^7 \text{ M}^{-1} \text{s}^{-1}$ ), confirming that FV<sub>a2</sub> is the better cofactor on a membrane even when only one bond is cut. The rate for the FX<sub>a</sub>–FV<sub>a2</sub> complex on a membrane is the same as the rate seen for the C6PS-assembled FX<sub>a</sub>–FV<sub>a2</sub> complex ( $2.5 \times 10^8 \text{ M}^{-1} \text{s}^{-1}$ ).

## DISCUSSION

Our results show that, when the more active factor V<sub>a</sub> isoform is used for membrane-based and solution-phase prothrombin activation by factor X<sub>a</sub>, the solution reaction is similar in overall rate and in reaction pathways to membrane-mediated activation. The C6PS and membrane complexes are similar in all respects: (1) they both cause significant fractions (58% for C6PS and 50–60% for membranes) of prothrombin to be converted directly (processively) to thrombin; (2) they both direct activation nearly exclusively through the MzII<sub>a</sub> intermediate; and (3) they both result in activation at nearly the same overall rate. Finally, because the rate of MzII<sub>a</sub> conversion to thrombin is roughly the same as the rate of reaction E, nearly all thrombin that is initially formed by the C6PS-assembled complex is formed via reaction E (channeling; Figure 3B), just as for the membrane complex (25). These results show that a membrane surface is not needed for efficient activation of prothrombin and thus provide strong support for the “regulatory PS hypothesis” that we have put forward to explain the origin of the rate enhancement by PS-containing membranes.

We are obliged to comment on a recent paper by Stone and Nelsestuen reporting the opposite conclusion to ours, namely, that C6PS does not trigger an efficient human prothrombinase at low concentrations but does trigger some



increase in prothrombinase activity between 250 and 500  $\mu\text{M}$  C6PS, presumably because of micelle formation (19). We believe these differences in conclusions to derive primarily from two sources. First, these authors used 5-fold lower  $\text{FX}_a$  and  $\text{FV}_a$  concentrations than we have used and did not pretreat cuvettes with these proteins prior to measurements. The two labs that have documented the interaction between factors  $\text{X}_a$  and  $\text{V}_a$  in the absence of membranes both report that pretreatment is required to reproducibly monitor the interaction (16, 45). Presumably, pretreatment followed by rinsing with buffer limits protein adsorption to glass surfaces during experiments, an artifact likely to be most significant at low protein concentrations. Second, we have always used 0.6 wt % PEG and not bovine serum albumin as a protein-stabilizing agent, because we noted early in our studies how sensitive C6PS cmc is to the protein concentration (9). Stone and Nelsestuen were correct in suggesting that the increase in prothrombinase activity that they observed between 250 and 500  $\mu\text{M}$  C6PS was due to micelle formation but were incorrect in suggesting that their observation, made in the presence of 15  $\mu\text{M}$  BSA, implies micelle formation under our conditions. We used quasi-elastic light scattering to measure the cmc of C6PS at the BSA concentration used by Stone and Nelsestuen and found, in agreement with their activity results, a value of 250–300  $\mu\text{M}$ . The same method reports a C6PS cmc of 700–750  $\mu\text{M}$  under our conditions. Another minor difference between our studies and those of Stone and Nelsestuen is that they used human  $\text{FV}_a$  in their experiments, while we used  $\text{FV}_{a2}$ , which is a better cofactor for  $\text{FX}_a$  (see the Results). However, this difference cannot explain the dramatic difference between our results, in that native  $\text{FV}_a$  is roughly  $2/3$   $\text{FV}_{a2}$ ; therefore, Stone and Nelsestuen should still have seen plenty of activity were it not for the issues described above. We conclude that the experiments of Stone and Nelsestuen were carried out under conditions that limit the formation of a soluble  $\text{FX}_a$ – $\text{FV}_{a2}$  complex but that favor condensation and stabilization of the  $\text{FX}_a$ – $\text{FV}_a$  complex on C6PS–BSA aggregates, leading to an unfortunate misinterpretation of our earlier results and to the clear difference between our conclusions.

Thus, what of the “surface dimensionality-reduction hypothesis”? It is reasonable to expect some rate enhancement because of the sequestering of the enzyme–cofactor complex and the substrate on a membrane. Our results also address this issue. First, the solution and membrane complexes are nearly identical with respect to the single-step activation of  $\text{MzII}_a$  to thrombin. Second, the extent of channeling is nearly identical for the membrane- and C6PS-assembled complexes. On the basis of these two observations, the 2-fold increase in the overall activation rate for the membrane complex relative to the solution complex must reflect slightly improved delivery of membrane-bound prothrombin to the membrane-bound complex on the membrane surface. Thus, there is an effect of surface dimensionality reduction, as previously proposed (2, 6, 8), but the magnitude of this effect is much smaller than has generally been assumed.

If PS-containing membranes do not exert their effect on prothrombin activation by “dimensionality reduction”, what is the origin of the effects of molecular PS that are documented in Table 1? It has long been known that PS-containing membranes lower the apparent  $K_M$  of prothrom-

binase (2), an argument in favor of improved substrate delivery on a surface. However, the complexities of the reaction scheme shown in Figure 1 obscure the meaning of an apparent  $K_M$  for the overall reaction. Because prothrombin and  $\text{MzII}_a$  adopt very different conformations on a PS-containing membrane (46), we cannot assume that  $K_M$  values applicable to one reaction in the scheme apply to others.  $\text{MzII}_a$  activation is the only single-step reaction for which we have rough  $K_M$  and  $k_{\text{cat}}$  values for both C6PS- and membrane-assembled complexes (reaction D in Table 1). We have estimated the  $K_M$  for  $\text{MzII}_a$  activation by  $\text{FX}_a$  alone (no membranes and no  $\text{V}_a$ ) as  $>10$   $\mu\text{M}$  with  $k_{\text{cat}}/K_M \sim 1100$   $\text{M}^{-1} \text{s}^{-1}$  (14), clearly not an impressive enzyme. However, factor  $\text{X}_a$ , when induced to bind to  $\text{FV}_{a2}$  by molecular PS, becomes a remarkably efficient enzyme, with  $K_M$  lowered to  $\sim 0.7$   $\mu\text{M}$  (Figure 3) and  $k_{\text{cat}}/K_M$  ( $\sim 2.7 \times 10^8$   $\text{M}^{-1} \text{s}^{-1}$ , Table 1) increased by  $10^5$ – $10^6$ -fold and approaching the expected diffusion limit for an enzyme ( $10^9$   $\text{M}^{-1} \text{s}^{-1}$ ). C6PS alone (i.e., without  $\text{V}_{a2}$ ) does not decrease  $K_M$  to a large extent ( $K_M > 2$   $\mu\text{M}$ ) and increases  $k_{\text{cat}}/K_M$  by  $\sim 600$ -fold (11). The C6PS-assembled prothrombinase has a  $k_{\text{cat}}/K_M$  another  $\sim 500$ -fold greater than C6PS-activated  $\text{FX}_a$ . Thus, molecular PS acts both as a cofactor that increases the catalytic efficiency of factor  $\text{X}_a$  and as a regulator molecule that triggers tight association between factors  $\text{X}_a$  and  $\text{V}_a$ . On the basis of these kinetic constants, C6PS and factor  $\text{V}_a$  are comparably important cofactors for factor  $\text{X}_a$ . However, the ability of  $\text{FV}_a$  to bind to  $\text{FX}_a$  and perform its cofactor role depends upon the binding of molecular PS to a regulator site on  $\text{FV}_a$  (18). This enzyme (the C6PS-assembled prothrombinase) has essentially the same  $K_M$  for  $\text{MzII}_a$  as the membrane-assembled enzyme ( $\sim 0.9$   $\mu\text{M}$ ) (25), the same  $k_{\text{cat}}/K_M$  ( $\sim 3 \times 10^8$   $\text{M}^{-1} \text{s}^{-1}$  with  $\text{FV}_{a2}$  as the cofactor), and thus the same  $k_{\text{cat}}$  ( $\sim 27$   $\text{s}^{-1}$ ).

The role of the platelet membrane in blood coagulation has been debated for years. Our results using soluble C6PS to replace a PS-containing membrane show that the PS molecule and not a membrane surface regulates the assembly, the activity, and the reaction mechanism of the human prothrombinase complex. Because C6PS is clearly not a natural lipid, does this have any relevance to the role of platelet membranes *in vivo*? First, our results imply that exposure of molecular PS on the surface of vesicles released by activated platelets (3, 4, 47) is a crucial step in regulating prothrombin activation during human blood coagulation. Second, given the high sequence homology of  $\text{FX}_a$  and  $\text{FV}_a$  to factors  $\text{IX}_a$  and  $\text{VIII}_a$ , it seems likely that PS exposure also regulates the activation of factor X by these proteins and may, for that matter, influence other membrane-dependent reactions of blood coagulation. We are testing this possibility, and if found to be the case, this would make PS a key second messenger in blood coagulation (48), with activated platelet vesicles exposing this regulatory molecule. Clearly, the platelet membrane surface must also play a critical role in blood coagulation beyond exposing PS, but our results suggest that we may need to look beyond its effect on individual proteolytic reactions to understand other aspects of the role of the platelet membrane (49).

## REFERENCES

1. Mann, K. G., Nesheim, M. E., Church, W. R., Haley, P., and Krishnaswamy, S. (1990) Surface-dependent reactions of the vitamin K-dependent enzyme complexes, *Blood* 76, 1–16.

2. Rosing, J., Tans, G., Govers-Riemslog, J., Zwaal, R., and Hemker, H. (1980) The role of phospholipids and factor Va in the prothrombinase complex, *J. Biol. Chem.* 255, 274–283.
3. Sandberg, H., Bode, A. P., Dombrose, F. A., Hoechli, M., and Lentz, B. R. (1985) Expression of coagulant activity in human platelets: Release of membranous vesicles providing platelet factor 1 and platelet factor 3, *Thromb. Res.* 39, 63–79.
4. Bevers, E. M., Roland, P. C., Tilly, H. J., and Zwaal, R. F. A. (1991) Transbilayer movement of procoagulant phospholipids during platelet microvesicle formation, *Throm. Haemostasis* 65, 688a.
5. Bevers, E. M., Comfurius, P., and Zwaal, R. F. (1983) Changes in membrane phospholipid distribution during platelet activation, *Biochim. Biophys. Acta* 736, 57–66.
6. Nesheim, M. E., Tracy, R. P., and Mann, K. G. (1984) “Clotspeed”, a mathematical simulation of the functional properties of prothrombinase, *J. Biol. Chem.* 259, 1447–1453.
7. Krishnaswamy, S., Jones, K. C., and Mann, K. G. (1988) Prothrombinase complex assembly. Kinetic mechanism of enzyme assembly on phospholipid vesicles, *J. Biol. Chem.* 263, 3823–3834.
8. Giesen, P. L., Willems, G. M., and Hermens, W. T. (1991) Production of thrombin by the prothrombinase complex is regulated by membrane-mediated transport of prothrombin, *J. Biol. Chem.* 266, 1379–1382.
9. Koppaka, V., Wang, J., Banerjee, M., and Lentz, B. R. (1996) Soluble phospholipids enhance factor Xa-catalyzed prothrombin activation in solution, *Biochemistry* 35, 7482–7491.
10. Srivastava, A., Quinn-Allen, M. A., Kim, S. W., Kane, W. H., and Lentz, B. R. (2001) Soluble phosphatidylserine binds to a single identified site in the C2 domain of human factor Va, *Biochemistry* 40, 8246–8255.
11. Banerjee, M., Majumder, R., Weinreb, G., Wang, J., and Lentz, B. R. (2002) Role of procoagulant lipids in human prothrombin activation. 2. Soluble phosphatidylserine upregulates and directs factor X(a) to appropriate peptide bonds in prothrombin, *Biochemistry* 41, 950–957.
12. Banerjee, M., Drummond, D. C., Srivastava, A., Daleke, D., and Lentz, B. R. (2002) Specificity of soluble phospholipid binding sites on human factor Xa, *Biochemistry* 41, 7751–7762.
13. Srivastava, A., Wang, J., Majumder, R., Rezaie, A. R., Stenflo, J., Esmon, C. T., and Lentz, B. R. (2002) Localization of phosphatidylserine binding sites to structural domains of factor Xa, *J. Biol. Chem.* 277, 1855–1863.
14. Wu, J. R., Zhou, C., Majumder, R., Powers, D. D., Weinreb, G., and Lentz, B. R. (2002) Role of procoagulant lipids in human prothrombin activation. 1. Prothrombin activation by factor Xa in the absence of factor Va and in the absence and presence of membranes, *Biochemistry* 41, 935–949.
15. Zhai, X., Srivastava, A., Drummond, D. C., Daleke, D., and Lentz, B. R. (2002) Phosphatidylserine binding alters the conformation and specifically enhances the cofactor activity of bovine factor Va, *Biochemistry* 41, 5675–5684.
16. Majumder, R., Weinreb, G., Zhai, X., and Lentz, B. R. (2002) Soluble phosphatidylserine triggers assembly in solution of a prothrombin-activating complex in the absence of a membrane surface, *J. Biol. Chem.* 277, 29765–29773.
17. Majumder, R., Wang, J., and Lentz, B. R. (2003) Effects of water soluble phosphatidylserine on bovine factor Xa: Functional and structural changes plus dimerization, *Biophys. J.* 84, 1238–1251.
18. Majumder, R., Quinn-Allen, M. A., Kane, W. H., and Lentz, B. R. (2005) The phosphatidylserine binding site of the factor Va C2 domain accounts for membrane binding but does not contribute to the assembly or activity of a human factor Xa-factor Va complex, *Biochemistry* 44, 711–718.
19. Stone, M. D., and Nelsestuen, G. L. (2005) Efficacy of soluble phospholipids in the prothrombinase reaction, *Biochemistry* 44, 4037–4041.
20. Rosing, J., and Tans, G. (1988) Meizothrombin, a major product of factor Xa-catalyzed prothrombin activation, *Thromb. Haemostasis* 60, 355–360.
21. Esmon, C. T., and Jackson, C. M. (1974) The conversion of prothrombin to thrombin. IV. The function of the fragment 2 region during activation in the presence of factor V, *J. Biol. Chem.* 249, 7791–7797.
22. Nesheim, M. E., and Mann, K. G. (1983) The kinetics and cofactor dependence of the two cleavages involved in prothrombin activation, *J. Biol. Chem.* 258, 5386–5391.
23. Krishnaswamy, S., Church, W. R., Nesheim, M. E., and Mann, K. G. (1987) Activation of human prothrombin by human prothrombinase. Influence of factor Va on the reaction mechanism, *J. Biol. Chem.* 262, 3291–3299.
24. Boskovic, D. S., Bajzar, L. S., and Nesheim, M. E. (2001) Channeling during prothrombin activation, *J. Biol. Chem.* 276, 28686–28693.
25. Weinreb, G. E., Mukhopadhyay, K., Majumder, R., and Lentz, B. R. (2003) Cooperative roles of factor Va and phosphatidylserine-containing membranes as cofactors in prothrombin activation, *J. Biol. Chem.* 278, 5679–5684.
26. Pei, G., and Lentz, B. R. (1991) Isolation and autolysis of human meizothrombin in the presence of dansylarginine-N-(3-ethyl-1,5-pentanedyl)amide, *Blood Coagulation Fibrinolysis* 2, 309–316.
27. Kane, W. H., and Majerus, P. W. (1981) Purification and characterization of human coagulation factor V, *J. Biol. Chem.* 256, 1002–1007.
28. Cutsforth, G. A., Koppaka, V., Krishnaswamy, S., Wu, J. R., Mann, K. G., and Lentz, B. R. (1996) Insights into the complex association of bovine factor Va with acidic-lipid-containing synthetic membranes, *Biophys. J.* 70, 2938–2949.
29. Krishnaswamy, S., Russell, G. D., and Mann, K. G. (1989) The reassociation of factor Va from its isolated subunits, *J. Biol. Chem.* 264, 3160–3168.
30. Hoekema, L., Nicolaes, G. A., Hemker, H. C., Tans, G., and Rosing, J. (1997) Human factor Va1 and factor Va2: Properties in the procoagulant and anticoagulant pathways, *Biochemistry* 36, 3331–3335.
31. Kim, S. W., Ortel, T. L., Quinn-Allen, M. A., Yoo, L., Worfolk, L., Zhai, X., Lentz, B. R., and Kane, W. H. (1999) Partial glycosylation at asparagine-2181 of the second C-type domain of human factor V modulates assembly of the prothrombinase complex, *Biochemistry* 38, 11448–11454.
32. Lentz, B. R., McIntyre, G. F., Parks, D. J., Yates, J. C., and Massenburg, D. (1992) Bilayer curvature and certain amphipaths promote poly(ethylene glycol)-induced fusion of dipalmitoylphosphatidylcholine unilamellar vesicles, *Biochemistry* 31, 2643–2653.
33. Haque, M. E., Das, A. R., and Moulik, S. P. (1995) Behaviors of sodium deoxycholate (Nad) and polyoxyethylene tert-octylphenyl ether (Triton X-100) at the air/water interface and in the bulk, *J. Phys. Chem.* 99, 14032–14038.
34. Haque, M. E., Das, A. R., and Moulik, S. P. (1999) Mixed micelles of sodium deoxycholate and polyoxyethylene sorbitan monooleate (Tween 80), *J. Colloid Interface Sci.* 217, 1–7.
35. Nesheim, M. E., Prendergast, F. G., and Mann, K. G. (1979) Interactions of a fluorescent active-site-directed inhibitor of thrombin: Dansylarginine N-(3-ethyl-1,5-pentanedyl)amide, *Biochemistry* 18, 996–1003.
36. Nesheim, M. E., Taswell, J. B., and Mann, K. G. (1979) The contribution of bovine factor V and factor Va to the activity of prothrombinase, *J. Biol. Chem.* 254, 10952–10962.
37. Rosing, J., Zwaal, R. F., and Tans, G. (1986) Formation of meizothrombin as intermediate in factor Xa-catalyzed prothrombin activation, *J. Biol. Chem.* 261, 4224–4228.
38. Laemmli, U. K. (1970) Cleavage of structural proteins during the assembly of the head of bacteriophage T4, *Nature* 227, 680–685.
39. Mitra, P., Pal, A. K., Basu, D., and Hati, R. N. (1994) A staining procedure using Coomassie brilliant blue G-250 in phosphoric acid for detection of protein bands with high resolution in polyacrylamide gel and nitrocellulose membrane, *Anal. Biochem.* 223, 327–329.
40. Krishnaswamy, S. (1990) Prothrombinase complex assembly. Contributions of protein–protein and protein–membrane interactions toward complex formation, *J. Biol. Chem.* 265, 3708–3718.
41. Vossen, K. M., Stickle, D. F., and Fried, M. G. (1996) The mechanism of CAP-lac repressor binding cooperativity at the *E. coli* lactose promoter, *J. Mol. Biol.* 255, 44–54.
42. van Holde, K. E., Johnson, W. C., and Ho, P. S. *Principles of Physical Biochemistry*, Vol. 17, pp 216–220, Prentice Hall, Upper Saddle River, NJ.
43. Ferguson, K. A. (1964) Ferguson plot analysis, *Metabolism* 13, 985–1002.
44. Leytus, S. P., Foster, D. C., Kurachi, K., and Davie, E. W. (1986) Gene for human factor X: A blood coagulation factor whose gene organization is essentially identical with that of factor IX and protein C, *Biochemistry* 25, 5098–5102.
45. Boskovic, D. S., Giles, A. R., and Nesheim, M. E. (1990) Studies of the role of factor Va in the factor Xa-catalyzed activation of



- prothrombin, fragment 1.2-prethrombin-2, and dansyl-L-glutamyl-glycyl-L-arginine-meizothrombin in the absence of phospholipid, *J. Biol. Chem.* 265, 10497–10505.
46. Chen, Q., and Lentz, B. R. (1997) Fluorescence resonance energy transfer study of shape changes in membrane-bound bovine prothrombin and meizothrombin, *Biochemistry* 36, 4701–4711.
47. Sims, P. J., Wiedmer, T., Esmon, C. T., Weiss, H. J., and Shattil, S. J. (1989) Assembly of the platelet prothrombinase complex is linked to vesiculation of the platelet plasma membrane. Studies in Scott syndrome: An isolated defect in platelet procoagulant activity, *J. Biol. Chem.* 264, 17049–17057.
48. Lentz, B. R. (2003) Exposure of platelet membrane phosphatidylserine regulates blood coagulation, *Prog. Lipid Res.* 42, 423–438.
49. Monroe, D. M., Hoffman, M., and Roberts, H. R. (2002) Platelets and thrombin generation, *Arterioscler., Thromb., Vasc. Biol.* 22, 1381–1389.

BI051469F